AGU PUBLICATIONS

Water Resources Research

RESEARCH ARTICLE
10.1002/2016WR019856

Key Points:
- Distance-based similarity captured spatial differences, correlation-based similarity temporal differences in groundwater dynamics
- Landscape position explained a larger portion of the variability in distance-based groundwater similarity than spatial distance
- Topographic indices were good predictors of groundwater similarity and allow upscaling groundwater dynamics to the catchment scale

Correspondence to:
M. Rinderer,
michael.rinderer@gmx.net

Citation:
Rinderer, M., B. L. McGlynn, and H. J. van Meerveld (2017), Groundwater similarity across a watershed derived from time-warped and flow-corrected time series, *Water Resour. Res.*, *53*, 3921–3940, doi:10.1002/2016WR019856.

Received 26 SEP 2016
Accepted 23 FEB 2017
Accepted article online 2 MAR 2017
Published online 15 MAY 2017

Groundwater similarity across a watershed derived from time-warped and flow-corrected time series

M. Rinderer[1,2], B. L. McGlynn[1], and H. J. van Meerveld[3]

[1]Nicholas School of the Environment, Duke University, Durham, North Carolina, USA, [2]Chair of Hydrology, University of Freiburg, Freiburg, Germany, [3]Department of Geography, University of Zurich, Zurich, Switzerland

Abstract Information about catchment-scale groundwater dynamics is necessary to understand how catchments store and release water and why water quantity and quality varies in streams. However, groundwater level monitoring is often restricted to a limited number of sites. Knowledge of the factors that determine similarity between monitoring sites can be used to predict catchment-scale groundwater storage and connectivity of different runoff source areas. We used distance-based and correlation-based similarity measures to quantify the spatial and temporal differences in shallow groundwater similarity for 51 monitoring sites in a Swiss prealpine catchment. The 41 months long time series were preprocessed using Dynamic Time-Warping and a Flow-corrected Time Transformation to account for small timing differences and bias toward low-flow periods. The mean distance-based groundwater similarity was correlated to topographic indices, such as upslope contributing area, topographic wetness index, and local slope. Correlation-based similarity was less related to landscape position but instead revealed differences between seasons. Analysis of variance and partial Mantel tests showed that landscape position, represented by the topographic wetness index, explained 52% of the variability in mean distance-based groundwater similarity, while spatial distance, represented by the Euclidean distance, explained only 5%. The variability in distance-based similarity and correlation-based similarity between groundwater and streamflow time series was significantly larger for midslope locations than for other landscape positions. This suggests that groundwater dynamics at these midslope sites, which are important to understand runoff source areas and hydrological connectivity at the catchment scale, are most difficult to predict.

1. Introduction

Groundwater is a major source of baseflow and also significantly contributes to streamflow during events [*McGlynn et al.*, 2004; *Tetzlaff et al.*, 2014]. Understanding catchment-scale groundwater dynamics is necessary for predicting how a catchment stores and releases water, which parts of the catchment are connected to the stream network via saturated flow, and which sources of water and pollutants influence stream water quantity and quality [*Asano et al.*, 2009; *Fischer et al.*, 2015]. However, groundwater monitoring is typically restricted to a few monitoring sites and their spacing and/or extent are limited (i.e., restricted to a few transects or a single hillslope). Groundwater measurements, therefore, typically do not capture the variability in groundwater dynamics at the catchment scale [*Bloeschl and Grayson*, 2000].

Several methods have been proposed to interpolate or extrapolate point-scale measurements to the catchment scale [*Bloeschl and Grayson*, 2000]. Some methods, such as Inverse Distance Weighting or Kriging, rely on the assumption that "... near things are more related than distant things" [*Tobler*, 1970, p. 236], thus assuming that spatial distance is a good criterion for interpolation. In contrast, observations show that groundwater and subsurface flow can be highly variable across a catchment [*Mosley*, 1979; *Sklash et al.*, 1986; *McDonnell*, 1990; *Rinderer et al.*, 2014] and that the characteristic length scale of groundwater levels is only in the order of a few to tens of meters [*Mosley*, 1982; *Lyon et al.*, 2006; *Tromp-van Meerveld and McDonnell*, 2006; *Bachmair et al.*, 2012].

Groundwater dynamics have been shown to vary depending on site characteristics [*McGlynn and McDonnell*, 2003; *Detty and McGuire*, 2010], such as land use and vegetation type [*Emanuel et al.*, 2014; *Bachmair et al.*, 2012] and soil type [*Tetzlaff et al.*, 2007; *Gannon et al.*, 2014; *Blumstock et al.*, 2016]. Geology and the properties of the aquifer also affect the spatial variability of the groundwater dynamics [*Tiedeman*

et al., 1998; *Winter et al*., 2008; *Kosugi et al*., 2008, 2011]. In catchments that are dominated by evapotranspiration or snowmelt, differences in the groundwater response have been related to elevation and aspect [*McMillan and Srinivasan*, 2015; *R. S. Smith et al*., 2014].

Groundwater dynamics can also be expected to be related to topography and landscape position as the local slope (or gradient) affects drainage and the upslope accumulated area affects the supply of water from upslope locations. Some simple distributed conceptual models, such as TOPMODEL [*Beven and Kirkby*, 1979], assume that the spatial pattern of groundwater levels is related to topography and studies have shown that simulations of the variable source area are in agreement with maps of the saturated area extent under wet catchment conditions [*Blazkova et al*., 2002; *Ali et al*., 2014]. Other studies found that near-stream sites (typically riparian or footslope locations) were the first to respond to rainfall events (but not always prior to streamflow), while the more distant wells in uphill locations exhibited delayed responses [*Seibert et al*., 1997; *Metcalfe and Buttle*, 2001; *Inamdar and Mitchell*, 2006; *Frisbee et al*., 2007; *Haught and van Meerveld*, 2011; *Detty and McGuire*, 2010]. The peak-to-peak lag times between groundwater and streamflow and their associated standard deviation also increased as a function of distance from the stream [*Haught and van Meerveld*, 2011; *von Freyberg et al*., 2014; *Blumstock et al*., 2016]. However, this behavior cannot be generalized since groundwater levels have also been observed to first respond in the upper hillslope [*Tromp-van Meerveld and McDonnell*, 2006; *Rodhe and Seibert*, 2011; *Penna et al*., 2015], or that groundwater in footslope and upslope locations responded earlier than in midslope locations [*van Meerveld et al*., 2015]. This variability can lead to spatial patterns of runoff contributing areas that differ between the falling and the rising limb of events [*Nippgen et al*., 2015].

In catchments with steep terrain and groundwater levels close to the soil surface, differences in groundwater dynamics have been attributed to small-scale morphological elements, such as of hollows and spurs [*Anderson and Burt*, 1978; *Bachmair and Weiler*, 2012; *Rinderer et al*., 2016]. In addition, groundwater levels and groundwater response timing have been related to topographically derived indices, such as the Topographic Wetness Index ($TWI = \ln(a/\tan\beta)$, where a is the upslope contributing area per unit contour length [m] and β is the local slope [°]) [*Beven and Kirkby*, 1979] in a number of studies [*Anderson and Burt*, 1978; *Burt and Butcher* 1985; *Troch et al*., 1993; *Lana-Renault et al*., 2014; *Rinderer et al*., 2014]. The upslope contributing area has also been shown to be a good predictor of hydrological connectivity [*Jencso et al*., 2009; *Jencso and McGlynn*, 2011; *Emanuel et al*., 2014; *Nippgen et al*., 2015]. However, in catchments with flatter topography or where groundwater levels are deeper, groundwater dynamics were not well correlated with surface topographic indices [*Barling et al*., 1994; *Seibert et al*., 1997; *Moore and Thompson*, 1996; *Buttle et al*., 2001]. In other studies, the correlation between groundwater levels and topographic indices was only significant during certain seasons, antecedent wetness conditions, or certain types of rain storms [*Dhakal and Sullivan*, 2014; *Bachmair and Weiler*, 2012].

A systematic investigation based on empirical data to test the hypothesis that sites in similar landscape positions or with similar site characteristics are characterized by similar groundwater dynamics is, however, still missing at the catchment scale. Similar groundwater behavior or *groundwater similarity* is here defined in terms of similarity in the response timing, amplitude, and shape of two groundwater time series and quantified by the cross correlation or the area (integral) between two time series. The main challenge is capturing the spatial-temporal variability in groundwater dynamics across an entire catchment. In addition, most previous studies on groundwater dynamics have analyzed maximum, mean, or median groundwater levels [*Rinderer et al*., 2014] or a sequence of snapshots [*Western and Grayson*, 1998; *Seibert et al*., 2003; *Ali et al*., 2011] or specific event response characteristics [*Rinderer et al*., 2016]. They have not analyzed the full dynamics of the groundwater time series. Here we present a systematic investigation of catchment-scale groundwater similarity based on empirical data comprising 41 months of groundwater time series from 51 monitoring sites. We analyzed the similarity between individual groundwater monitoring sites, as well as the similarity between the individual groundwater monitoring sites and streamflow at the catchment outlet to have a common reference for all sites. Specifically, we answer the following questions:

1. How similar are the groundwater table dynamics across a catchment?
2. Is groundwater similarity more strongly related to landscape position or spatial distance?
3. Does groundwater similarity differ between seasons?

2. Methods

2.1. Study Catchment

Groundwater similarity was studied in a 20 ha prealpine headwater catchment located 40 km southeast of Zurich, Switzerland (see Figure 1). The high annual average precipitation of 2300 mm/yr (of which one third falls as snow) causes wetness conditions to be high throughout the year [*Feyen et al*., 1999]. The elevation in the catchment ranges from 1270 to 1650 m a.s.l. and the slopes are steep (average 35%). The drainage network is dense (21 km/km^2) but the catchment has a very limited riparian area. The steep hillslopes have a pronounced small-scale relief with gentle ridges and depressions, as well as sequences of flatter landscape units that originate from soil creeping and historic landslides. In these flatter areas moors with a thick organic soil horizon (up to 1 m thickness) have formed, while the steep hillslopes and ridge sites are typically forested (Picea abies L. with an understory of Vaccinium sp. [*Hagedorn et al*., 2000]). The mineral soil in the moors, where the water table is persistently close to the soil surface, is classified as a mollic Gleysol with typically a permanently reduced Bg horizon (43% clay, 42% silt, and 15% sand) [*Schleppi et al*., 1998]. At the steeper ridge locations, where the water table is normally more than 40 cm below the soil surface, the soils are classified as umbric Gleysol with an oxidized Bw horizon (49% clay, 46% silt, and 5% sand) [*Schleppi et al*., 1998; *Hagedorn et al*., 2000]. The hydraulic conductivity is typically high in the soil layers close to the soil surface and decreases rapidly with depth. Therefore, differences in the soil texture and thus storage properties between the two gleysols are not expected to vary much across the catchment and storage capacity is mainly dependent on antecedent wetness and soil depth. Soil depth is related to slope (Spearman rank correlation coefficient (r_s) = −0.44) and varies from 0.5 to 1 m at the ridge sites to 2.5 m in depressions. The geology is Flysch, a clay-rich and poorly draining bedrock with calcareous sandstone and argillite and bentonite schist layers [*Mohn et al*., 2000].

2.2. Field Measurements

Groundwater levels were recorded at 51 sites at a 5 min interval during the snow-free period (May until December) and a 10 min interval during the period with snow cover using Odyssey capacitance water level loggers (Dataflow Systems Pty Limited). In contrast to other studies that typically arrange their wells along transects or on a grid on a selected hillslope, the groundwater monitoring sites in this study were chosen to be a representative sample from the frequency distribution of the TWI in the catchment and to be representative for the different landscape positions and morphological units. They were thus distributed irregularly across the entire catchment [*Rinderer et al*., 2014]. The monitoring sites included 8 ridge sites, 22 midslope locations, and 21 footslope or depression locations. Twenty sites were forested and 31 were located in grassland; 25 had a mollic Gleysol and 26 had an umbric Gleysol. The wells were hand-augered to depth of

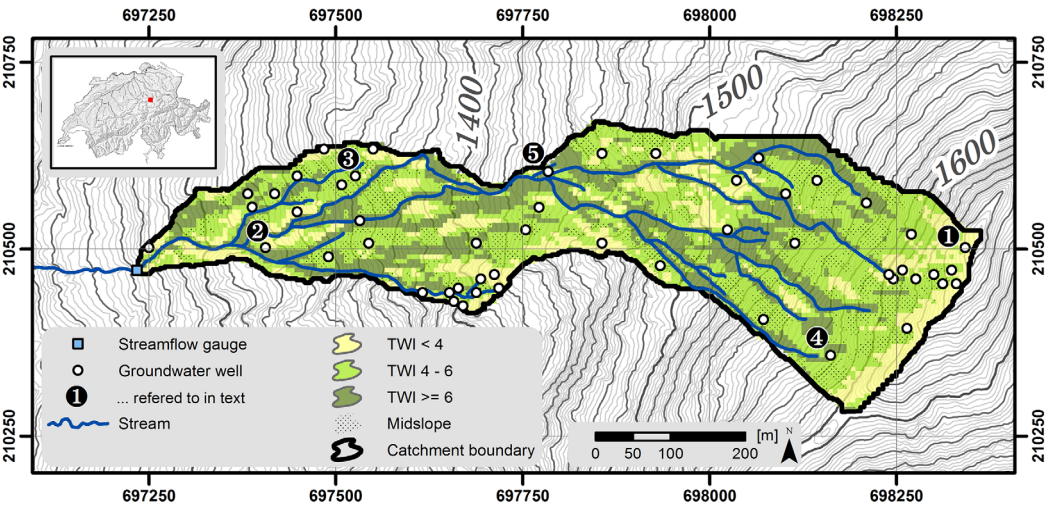

Figure 1. Map of the study catchment with the 51 groundwater monitoring sites and the spatial distribution of Topographic Wetness Index (TWI). Shaded areas are midslope locations with a TWI between 4 and 6, an upslope contributing area between 200 and 600 m^2 and a slope between 30 and 50%. Sites labeled with numbers 1–5 indicate wells that are mentioned in detail throughout the manuscript and are shown in Figures 3, 4, and 6.

refusal, which on average was 1.06 m below the surface, but ranged from 0.45 m at steep ridge sites to 2.16 m in footslope locations and depressions. The wells were screened over their entire length and sealed with bentonite at the soil surface to avoid surface runoff entering the wells.

Stream water level was measured at a 5 min interval at a natural cross section at the catchment outlet with a pressure transducer (DL/N 70 by STS, Sensor Technik Sirnach AG) during the snow-free period and at a 10 min interval during winter 2011 and 2012 using a capacitance water level logger (Odyssey). Stage was converted into streamflow using a site-specific rating curve based on salt dilution measurements that covered 58% of the range of observed stream water levels. For 1% of the 4 year study period the water level was higher than the measurements used to create the stage-discharge relationship. Changes in the natural cross section were documented monthly and were considered minor for the study period.

Precipitation, air temperature, and barometric pressure were measured at a meteorological weather station 1 km northwest of the catchment at 1219 m a.s.l. No reliable information on the spatial variability of the meteorological variables within the catchment are available for the study period but we assume that they are relatively small and that their influence on groundwater dynamics averages out over the monthly, seasonal, and annual timescales that are analyzed in this study.

2.3. Site Characteristics

To quantify the relation between groundwater similarity and landscape position, a set of local, upslope, and downslope site characteristics was used. These included local slope [*Tarboton*, 1997], local curvature [*Evans*, 1980; *Travis et al*., 1975], Topographic Wetness Index (TWI) [*Beven and Kirkby*, 1979], soil depth, the size, mean slope, mean curvature, and mean TWI of the upslope contributing area and the fraction of the upslope contributing area that is forested. To quantify spatial distance, the Euclidean distance among all groundwater monitoring sites, the Euclidean distance between all groundwater monitoring sites and the catchment outlet and the distance along the flow path from each groundwater monitoring location to the nearest stream was calculated using the D8-flow algorithm [*O'Callaghan and Mark*, 1984]. The surface topography based distance to the nearest stream is considered to be representative of the subsurface flow path to the nearest stream because the perched groundwater levels are shallow. Furthermore, no information about the bedrock topography or the topography of the soil layer where ponding occurs is available.

To be consistent with previous studies in the catchment [*Rinderer et al*., 2014, 2016] sites with a TWI >6, a local slope $<30\%$ and an upslope contributing area >600 m^2 are defined as typical footslope locations. Upslope locations are defined as sites with a TWI <4, a local slope $>50\%$, and an upslope contributing area <200 m^2, whereas midslope locations have a TWI between 4 and 6, a local slope between 30 and 50%, and an upslope contributing area between 200 and 600 m^2 (Figure 1).

All topographic indices were based on a 6 by 6 m Digital Terrain Model (DTM) obtained from LiDAR data (original resolution: 2 by 2 m) with an average point density of 1 point per 2 m^2. This resolution was deemed to be the best compromise between resolving the prevailing morphology that influences groundwater levels without being obscured by microtopography that largely affects the soil surface roughness. All topographic indices were calculated using the open source software SAGA-GIS [*Conrad*, 2006] and the triangular multiple flow direction algorithm [*Seibert and McGlynn*, 2007]. Soil depth was measured at each groundwater well during installation. The forested fraction of the upslope contributing area was derived from aerial photographs taken in 2007. Changes in forest cover extent between 2007 and the 2010–2014 study period were minor.

2.4. Similarity Measures

The similarity between two time series X(t) and Y(t) can be quantified by the sum of the distance (i.e., area) between the two time series (calculated by the integral between X(t) and Y(t) when $X(t) < Y(t)$ for all time steps) or the correlation between the two time series. The former, in the literature called *distance-based* similarity, is sensitive to differences in the shape and average level of two time series, while the *correlation-based* similarity measure is sensitive to differences in timing.

Suppose that two similar time series are shifted by a few time steps, then the area between them becomes large and the distance-based similarity measure indicates that the two time series are very different, even though they have a similar shape. Such shifts can be caused by interpolation of the data from loggers that measure the water level at a slightly different time or sensors that have a different measuring accuracy.

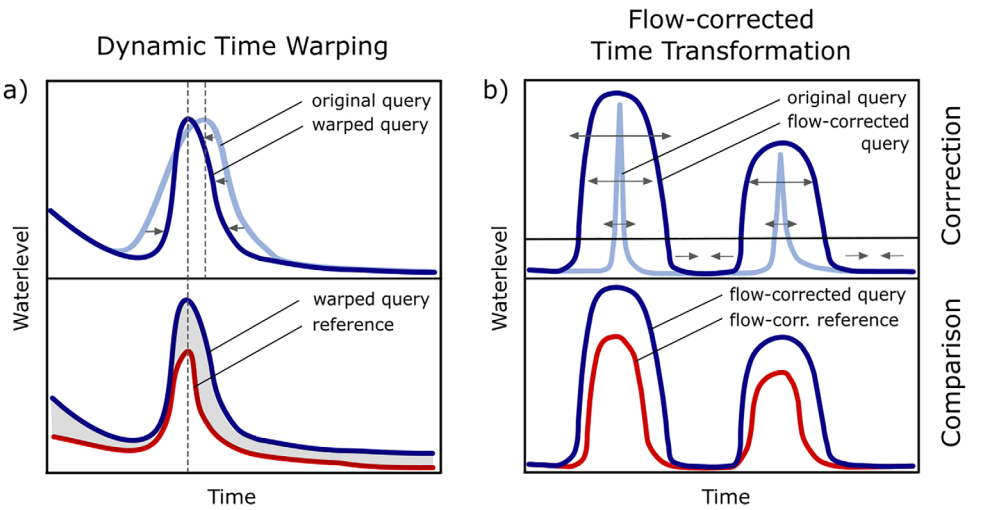

Figure 2. Schematic sketch of the basic concept of time warping and Flow-corrected Time Transformation. (a) Dynamic Time Warping comprises a controlled shifting and/or warping of the query time series (light blue) relative to a reference time series (red) to compensate for small shifts in time. The distance-based similarity (DTW) is then calculated between the warped query (dark blue) and the reference time series (red). (b) Correlation-based similarity measures (CFC) can have a bias toward long low-flow periods. To compensate for this effect, the Flow-corrected Time Transformation is applied whereby the length of the time steps of the query time series (light blue; e.g., groundwater values) is stretched or compressed in the time domain proportional to the streamflow values at the catchment outlet. This results in a flow-corrected query time series (dark blue) which is then compared to the flow-corrected reference (red) that has been processed with the same time transformation.

Dynamic Time Warping [*Sakoe and Chiba*, 1978] can be used to compensate for this drawback. The Dynamic Time-Warping algorithm allows for shrinking or stretching the time axis of Y(t), called *query*, in order to better match the timing of the reference time series X(t) (Figure 2a). The optimal degree of warping needs to be determined by an objective function. The classical Dynamic Time Warping algorithm [*Sakoe and Chiba*, 1978] optimizes the distance between two time series in a point-wise manner but can result in strong deformation artifacts that alter the shape of the original time series [*Bloemberg et al.*, 2013]. To address this, Correlation-optimized Time Warping is applied piecewise over segments and uses Pearson correlation as the objective function to determine the amount of time warping [*Nielsen et al.*, 1998]. For both optimization procedures, the warping needs to be restricted to a meaningful degree. In our analysis, a maximum of 30 min of warping was chosen to preserve the character of the warped time series and to prevent incorrect assignment of peaks. A more relaxed warping (i.e., maximum warping of several hours) increases the potential of wrong assignments of peaks in the query time series relative to the reference and would therefore potentially add an artificial error to the query. We added a constant offset to Y(t) before calculating the integral between the two time series in order to guarantee that $X(t) < Y(t)$ for all time series.

To quantify the similarity of two time series by their correlation, we used the Spearman rank correlation coefficient. Because recession and low-flow periods often dominate a time series, the correlation coefficient can be biased toward these periods. However, for a better understanding of runoff generation processes and runoff source area dynamics, the groundwater response during events is more relevant than during the recession or baseflow periods. To avoid the bias toward low flows, it is useful to apply the Flow-corrected Time Transformation [*Rodhe et al.*, 1996; *Smith et al.*, 2014]. In our case this involved stretching the time axis of the specific discharge time series, measured at the catchment outlet, proportional to the specific discharge during periods with above-average specific discharge, and shrinking the time axis for all periods with below-average specific discharge (Figure 2b). This Flow-corrected Time Transformation based on the streamflow time series was applied to all groundwater time series in order to have the same correction for all time series.

2.5. Analysis Methods

The 5 min groundwater level data were normalized by the soil depth (determined during well installation) so that they range between zero when the groundwater level was at the soil-bedrock interface and 1 when the groundwater was at the soil surface. This normalization was used to make the groundwater levels more comparable between sites in terms of the fraction of the soil profile that is saturated and above all is a more

robust measure when the groundwater levels are transferred to sites where the soil depth is estimated or not known. All time series were subsampled to a 15 min time interval in order to reduce computational demand, while still reflecting the relatively flashy groundwater response. Only the data of the 41 months between 2010 and 2014 for which at least two thirds of all monitoring sites had data were included in the analyses.

Two sets of similarity measures were calculated: (1) *DTW*: the distance-based similarity measure applied to groundwater levels normalized by soil depth that had been preprocessed using Dynamic Time Warping (objective function: Pearson correlation between two time series) and (2) *CFC*, the correlation-based similarity measure applied to flow-corrected groundwater level data. It is useful to consider both similarity measures as a high distance-based similarity (DTW) but intermediate to low correlation-based similarity (CFC) between two groundwater level time series suggests that the two sites are similar in magnitude and shape of the groundwater dynamics but differ in terms of response timing. In a similar way, a high correlation-based similarity (CFC) but intermediate to low distance-based similarity (DTW) suggests that the groundwater levels are similar in response timing but not in magnitude of the response. In addition to the two similarity measures, we also tested the classical Dynamic Time Warping (objective function: minimum sum of distance between the two time series) but this algorithm resulted in stronger warping artifacts than DTW. Since the conclusions drawn from the analyses using the classic Dynamic Time Warping and DTW did not differ considerably, only the latter results are presented in this paper.

Both similarity measures were calculated for all possible pairs of groundwater monitoring sites and between each groundwater monitoring location and the specific discharge at the catchment outlet to compare the differences in groundwater dynamics to one common reference. All analyses were also performed for the stream water level time series (instead of specific discharge) but since the results and the conclusions drawn from the analyses using water level did not differ from those based on streamflow, only the results for the specific discharge are presented because they can be more easily compared with and transferred to other sites.

DTW-based similarity was calculated using the MATLAB function of *Skov et al*. [2006] with segment length (t) equal to 144 time steps and a maximum warping or slack (m) equal to 2 time steps. All other data preprocessing and data analyses were done in R (R Developer Community) using functions from the *stats*-package to calculate the CFC-based similarity and the *dtw*-package [*Giorgino*, 2009] for calculating the classical Dynamic Time Warping.

The DTW-based similarity was calculated for each of the 41 months individually in order to avoid strong artifacts of the warping algorithm that are typical for long time series [*Tomasi et al*., 2004]. Because the distance-based measures are additive, it was possible to aggregate the DTW-based similarity to longer periods. This was done for three periods: the growing season from the beginning of June until the end of September, the dormant season between the beginning of October and the end of January and the spring and snowmelt season between the beginning of February and the end of May. In addition, the DTW-based similarity was also aggregated for the months with snow cover (22) and without snow cover (19) based on snow records. The CFC-based similarity is not additive and was calculated separately for the individual months, and seasons. The time spans of the flow-corrected months were selected to cover the same events that were included in the corresponding month in the raw data. Differences in the CFC- and DTW-based similarities for the different seasons and the months with and without snow cover were tested for statistical significance using the Mann-Whitney test ($\alpha = 0.05$).

Groundwater similarity measures were rescaled to range from 1 (most similar) to 0 (least similar). To achieve this, the DTW-based similarity was normalized by the minimum and maximum similarity of the entire data set considering all pairs of sites and all months. For the CFC-based similarity, all negative correlations were set to zero before normalization. While this procedure neglects potential relations between two monitoring sites that occur with a certain time delay, the aim of this paper is to identify landscape positions with similar dynamics in terms of shape and response timing to allow upscaling of groundwater dynamics to nonmonitored sites in the catchment. Negative correlations mean that one time series is rising, while at the same time the other time series is falling, which indicates that the response behavior of the two sites to rainfall is different. The way the CFC-based similarity values are normalized (i.e., setting all values <0 to zero) allows to intuitively interpret them as positive correlation coefficients. Furthermore, using the same range of values (0-1) for the distance-based and correlation-based similarity allows better comparison between them.

Analysis of variance (ANOVA) was performed to quantify the joint and partial effect of landscape position and spatial distance on the spatial variability of the mean similarity between each groundwater time series and the streamflow time series at the catchment outlet for each of the 41 months. For the comparison between groundwater and streamflow dynamics the Euclidean distance between each groundwater monitoring location and the catchment outlet was chosen as a measure of spatial distance. The distance from each groundwater monitoring location to the nearest stream was considered as well but was found less informative as it lacks one common reference location. The TWI was chosen to represent landscape position because it is a topographic index that incorporates the local slope that represents the local drainage conditions and upslope contributing area that affects the water input form upslope. All other site characteristics that were not correlated to TWI were also examined in the ANOVA but were not significant in explaining the variability in the DTW- or CFC-based similarity.

Similarity among all pairs of groundwater monitoring sites as a function of landscape position and spatial distance was also analyzed. The DTW- and CFC-based similarities between all pairs were calculated. The pairs of sites were sorted according to their upslope contributing area, local slope, TWI, distance to the nearest stream, and Euclidean distance between the groundwater monitoring sites and bilinear interpolation was used to generate an equally spaced similarity matrix as the site characteristics were not evenly distributed over the total range of values. This resulted in sets of interpolated mean DTW- and CFC-based similarity matrices, which were symmetric, positive semidefinite with diagonal values equal to 1 and yielded exact interpolation results (i.e., interpolated values at the sampling locations are identical to the measurements that are used for the interpolation). Topographic site characteristic and spatial distance matrices were interpolated in the same way. Mantel tests [*Mantel*, 1967] were performed to quantify the Pearson correlation and its significance for all corresponding positions in the DTW- or CFC-based similarity matrices and the interpolated topographic and distance matrices. Technically the nonredundant portions of these matrices (e.g., the lower or upper triangle of symmetrical matrices, excluding the diagonals) are converted into column vectors and the correlation between these two vectors is calculated. For the ANOVA and the Mantel tests the R-package *vegan* was used, while the *fields*-package [*Nychka et al*., 2016] was used for calculating the Euclidean distance.

3. Results

3.1. Groundwater Dynamics and Landscape Position

The groundwater levels at the different landscape positions varied in the response frequency, response amplitude, and the rate of decline [*Rinderer et al*., 2016]. Figure 3 shows the groundwater time series of five

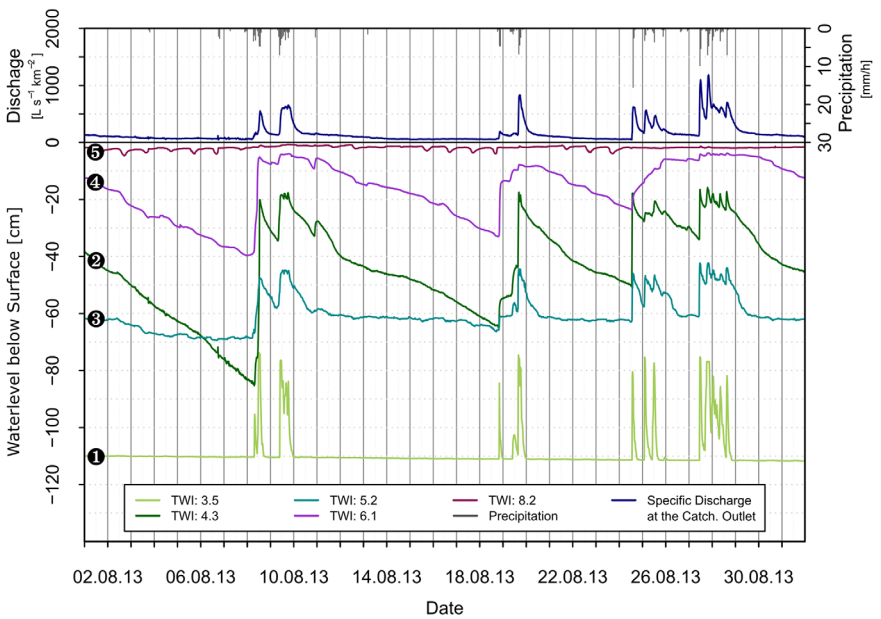

Figure 3. Groundwater time series of five selected monitoring sites with different values for the Topographic Wetness Index (TWI) for August 2013, a typical month in the growing season. The time series for these selected monitoring sites highlight the differences in the response timing, amplitude, and response frequency (see Figure 1 for the location of the wells).

representative monitoring sites in typical landscape positions that we highlight throughout the text. Sites with a TWI <4 (Figure 1) had a low mean groundwater level and responded less frequently but more sharply to rainfall events than the other sites. Sites with a TWI between 4 and 6 responded more frequently and showed high variability in the response amplitude. Sites with a TWI >6 typically had a small response amplitude since the water table remained close to the soil surface during most of the measurement period.

3.2. Similarity Between Groundwater and Streamflow

3.2.1. Distance-Based Similarity (DTW)

The spatial variability in the mean of the DTW-based similarity between the month-long groundwater level time series at a monitoring location and the streamflow time series at the catchment outlet was large (lower quartile = 0.26, median = 0.59, upper quartile = 0.82) and was related to landscape position (Figure 4a). Sites only a few meters apart from each other could show considerable differences in mean DTW-based similarity (Figure 4a). For all footslope locations the mean DTW-based similarity was >0.8, for the mid and upslope locations the mean DTW-based similarity ranged between 0.1 and 0.9 and for all steep ridge sites the mean DTW-based similarity was <0.4 (Figure 5).

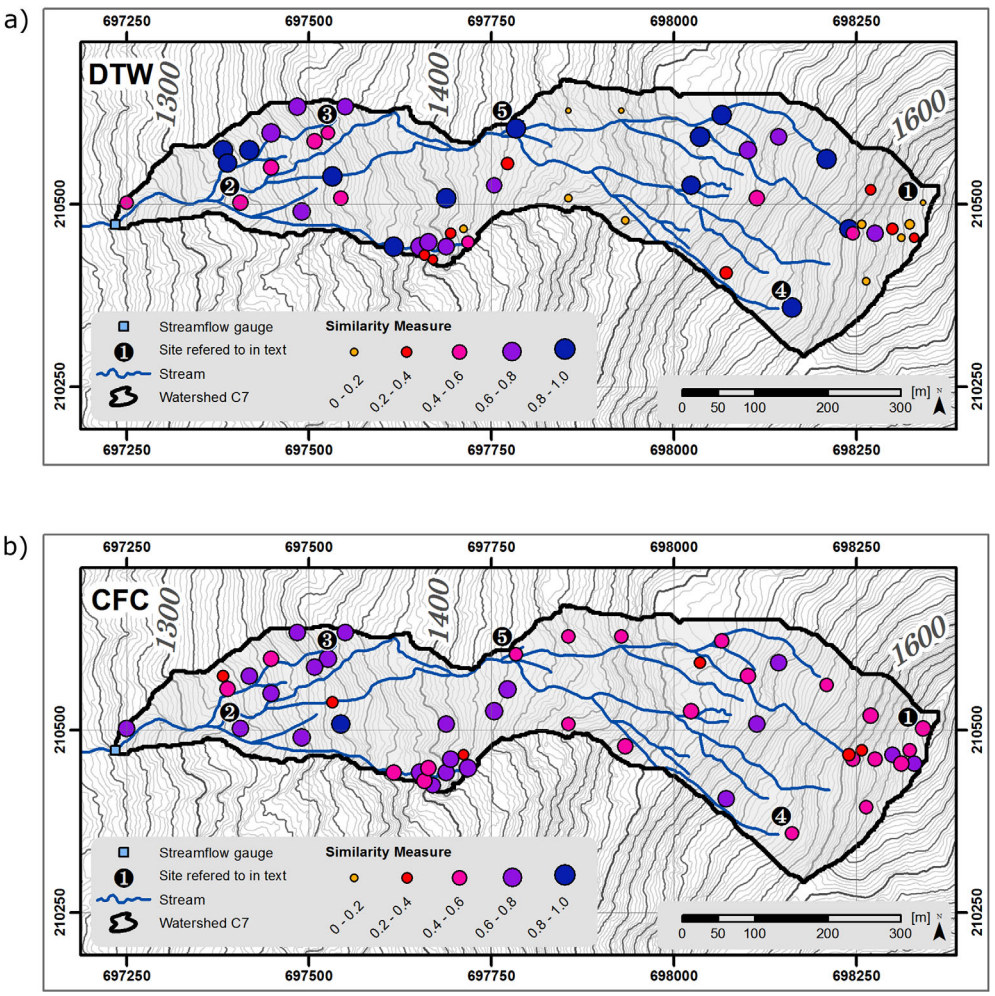

Figure 4. Maps of the mean similarity between groundwater and streamflow dynamics based on (a) distance-based similarity and Dynamic Time Warping (DTW) and (b) correlation-based similarity and Flow-corrected Time Transformation (CFC). A high distance-based similarity but intermediate to low correlation-based similarity suggests that the groundwater dynamic at the site is similar in magnitude and shape to the streamflow dynamic but differs in terms of timing. Similarly, a high correlation-based similarity but intermediate to low distance-based similarity suggests that groundwater and streamflow dynamic is similar in timing but differs in magnitude and shape.

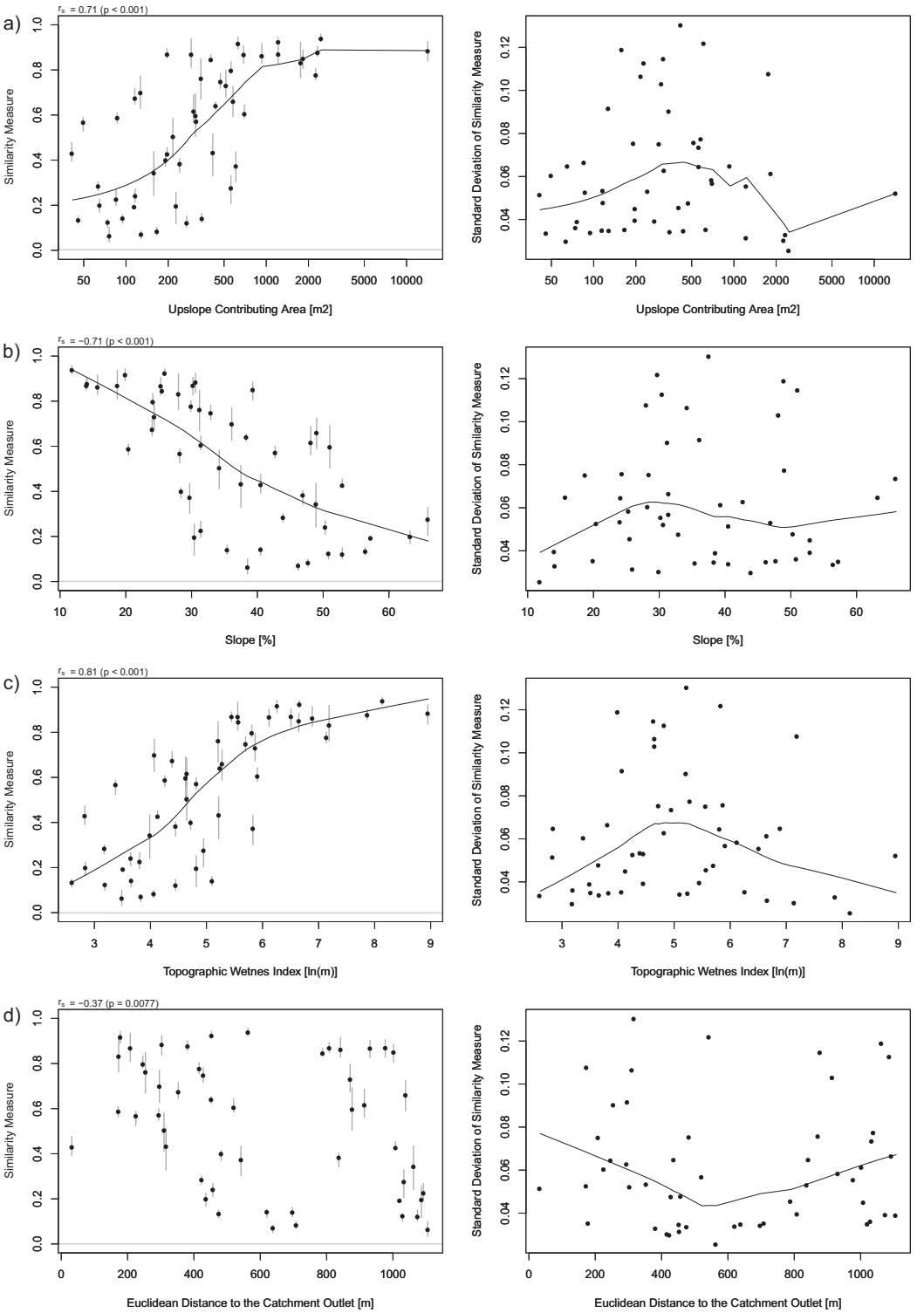

Figure 5. Mean (black dots) and Inter Quartile Range (bars) (left column) and standard deviation (right column) of DTW-based similarity of each month-long groundwater time series and the streamflow time series as a function of (a) upslope contributing area, (b) slope, (c) Topographic Wetness Index, and (d) Euclidean distance to the catchment outlet. The black line shows the LOWESS curve based on a locally weighted polynomial regression fitted to the median similarity values [*Cleveland*, 1979]. The plots show that DTW-based groundwater similarity is correlated with topographic indices (except for the Euclidean distance to the catchment outlet) and the high variability at midslope locations with an upslope contributing area between 200 and 600 m^2, a slope between 30 and 50% and TWI between 4 and 6.

The mean DTW-based similarity between each groundwater time series and the streamflow time series at the catchment outlet was significantly correlated with mean curvature of the upslope contributing area (Spearman rank correlation coefficient r_s: −0.82), TWI (r_s: 0.81), local slope (r_s: −0.71), upslope contributing area (r_s: 0.71), the mean TWI of the upslope contributing area (r_s: 0.62), the flow distance to the nearest stream (r_s: −0.35), and the soil depth (r_s: 0.33) (see Table 1 and Figure 5). The mean DTW-based similarity between the groundwater time series and the streamflow time series at the catchment outlet was also statistically significantly correlated with the Euclidean distance to the catchment outlet (r_s: −0.37; see Table 1 and Figure 5d) but the relationship was weaker than the correlation with the topographic site characteristics.

The standard deviation of the DTW-based similarity for the 41 months was small (mean = 0.06, lower quartile = 0.04, median = 0.05, upper quartile = 0.08) but significantly higher for midslope locations than for the footslope and upslope locations (p values of Mann-Whitney test: 0.01 and 0.004, respectively). The standard deviation of the DTW-based similarity for the 41 month was also significantly larger for sites with an intermediate distance to the nearest stream (e.g., 25–100 m, 22 sites) compared to all other sites that were either closer (<25 m, 13 sites) or further away (>100 m, 12 sites) from the stream ($p = 0.03$). In contrast, the standard deviation of the DTW-based similarity was significantly higher for sites with an Euclidean distance to the catchment outlet <350 m (13 sites) or >800 m (19 sites) than for sites with an intermediate Euclidean distance (19 sites) ($p < 0.001$) (see Figure 5d).

The frequency distribution of the DTW-based similarity between the groundwater time series for each monitoring location and the streamflow time series at the catchment outlet for all 41 months showed a distinct relation with site characteristics (Figure 6). Sites with a TWI <4 had predominantly positively skewed distributions of DTW-based similarity, which means that these sites had predominantly small DTW-based similarity values and their dynamics were thus different from the streamflow time series at the catchment outlet. The DTW-based similarity of sites with a TWI between 4 and 6 was distributed more uniformly or normally and sites with TWI >6 had predominantly high similarity values that were negatively skewed. These differences were even more pronounced when considering only the snow-free months and were still clearly evident, but less pronounced, when considering only the months with snow cover.

Table 1. Spearman Rank Correlation (Upper Triangle) and p Values (Lower Triangle) for the Relation Between the Mean DTW- and CFC-Based Similarity Between Groundwater and Streamflow and the Site Characteristics, Which Shows That the Distance-Based Similarity Measure (DTW) Is Correlated With Topographic Indices but the Correlation-Based Similarity Measure (CFC) Is Not, Except for the Euclidean Distance to the Outlet[a]

	Mean DTW	Mean CFC	Euclidean Distance to the Outlet	Local Slope	Mean Slope of the Upslope Contributing Area	Local Curvature	Mean Curvature of the Upslope Contributing Area	Upslope Contributing Area	Topographic Wetness Index (TWI)	Mean TWI of the Upslope Contributing Area	Flow Distance to the Stream	Forest Percentage of the Upslope Contributing Area	Soil Depth
Mean DTW		0.00	**−0.37**	**−0.71**	−0.24	−0.24	**−0.82**	**0.71**	**0.81**	**0.62**	**−0.35**	−0.08	**0.33**
Mean CFC	*0.87*		**−0.40**	−0.08	−0.27	−0.01	0.05	−0.06	−0.04	0.06	0.16	0.00	−0.02
Euclidean distance to the outlet	*<0.01*	*<0.01*		**0.40**	0.26	−0.09	0.15	0.05	−0.13	−0.15	0.17	**−0.28**	−0.09
Local slope	*<0.001*	*0.58*	*<0.01*		**0.61**	0.27	**0.61**	**−0.44**	**−0.64**	**−0.43**	0.08	0.07	**−0.44**
Mean slope of the upslope contributing area	*0.09*	*0.06*	*0.06*	*<0.001*		0.07	0.22	−0.07	−0.24	**−0.31**	−0.25	**0.38**	−0.23
Local curvature	*0.09*	*0.93*	*0.53*	*0.05*	*0.64*		**0.45**	**−0.48**	**−0.51**	−0.10	0.10	−0.13	0.09
Mean curvature of the upslope contributing area	*<0.001*	*0.74*	*0.30*	*<0.001*	*0.11*	*<0.01*		**−0.94**	**−0.97**	**−0.80**	0.26	0.15	−0.25
Upslope contributing area	*<0.001*	*0.67*	*0.74*	*<0.01*	*0.60*	*<0.001*	*<0.001*		**0.96**	**0.73**	−0.23	−0.15	0.16
Topographic Wetness Index (TWI)	*<0.001*	*0.76*	*0.36*	*<0.001*	*0.10*	*<0.001*	*<0.001*	*<0.001*		**0.73**	−0.24	−0.13	0.24
Mean TWI of the upslope contributing area	*<0.001*	*0.66*	*0.28*	*<0.01*	*0.03*	*0.50*	*<0.001*	*<0.001*	*<0.001*		−0.11	**−0.39**	0.21
Flow Distance to the stream	*0.01*	*0.27*	*0.24*	*0.58*	*0.08*	*0.49*	*0.06*	*0.11*	*0.08*	*0.45*		**−0.33**	0.14
Forest percentage of the upslope contributing area	*0.60*	*0.99*	*0.04*	*0.65*	*<0.01*	*0.36*	*0.29*	*0.29*	*0.36*	*<0.01*	*0.02*		−0.20
Soil depth	*0.02*	*0.89*	*0.53*	*<0.01*	*0.10*	*0.55*	*0.08*	*0.26*	*0.09*	*0.15*	*0.32*	*0.16*	

[a]Bold font: significant correlations, DTW: distance-based similarity and dynamic time warping, CFC: correlation-based similarity and flow-corrected time transformation.

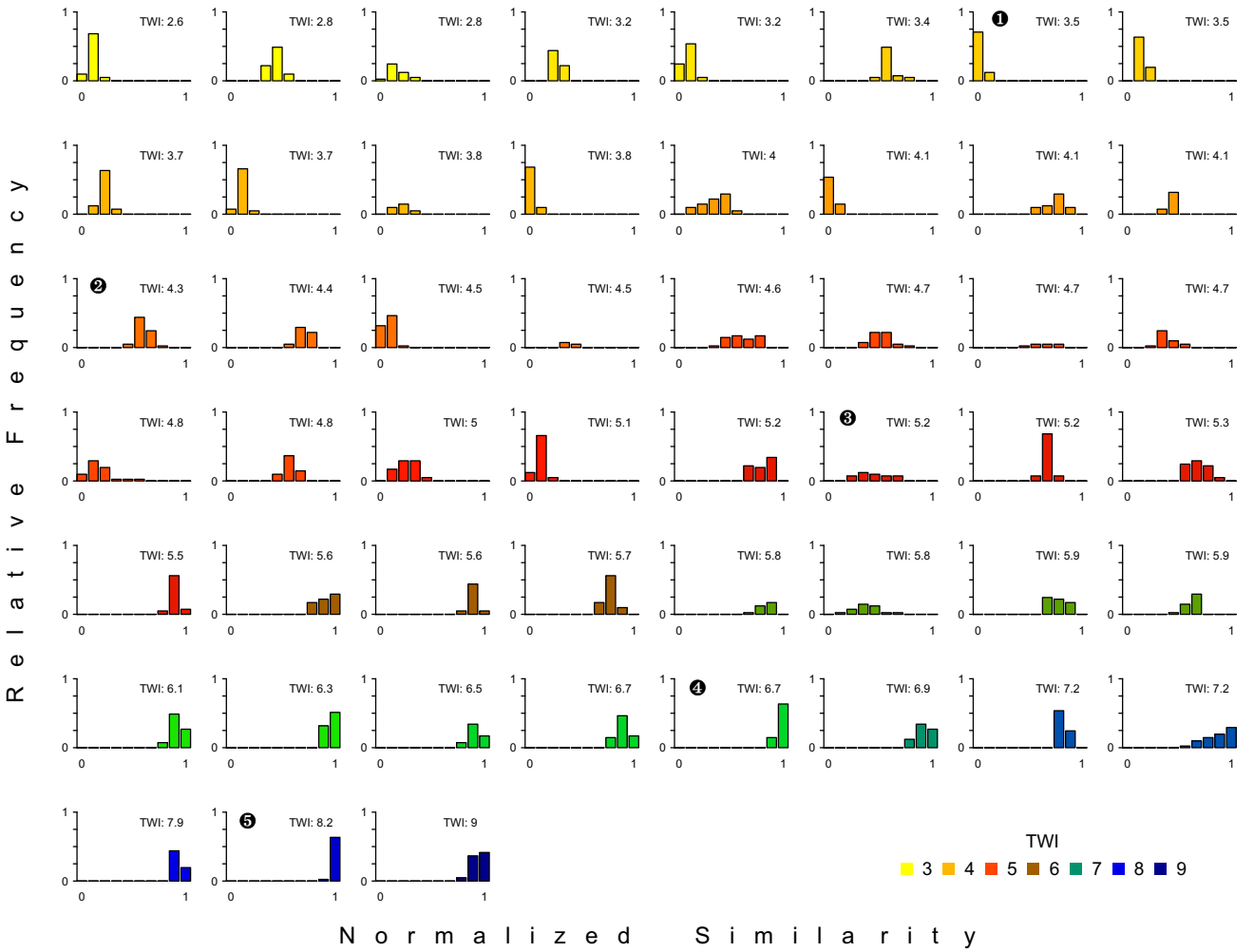

Figure 6. Relative frequency distributions of DTW-based similarity between the groundwater level time series at each monitoring site and the streamflow time series at the catchment outlet for all 41 calendar months, highlighting that the skewness of the groundwater similarity distribution is related to topography. Numbers in the upper right corner of each subplot indicate the TWI of the site; the location and time series of the representative monitoring sites (see number in black circle) can be seen in Figures 1 and 3.

None of the results for the mean and standard deviation of the DTW-based similarity relative to streamflow at the catchment outlet were significantly different when considering the months with and without snow cover, the months of the growing, dormant, and spring seasons or the months of each year between 2010 and 2014 separately ($p \gg 0.05$). The results for the median DTW-based similarity were also similar to the mean-DTW-based similarity.

3.2.2. Correlation-Based Similarity (CFC)

The CFC-based similarity was generally high (lower quartile = 0.46, median = 0.60, upper quartile = 0.65) and relatively similar across the catchment (see Figure 4b), indicating small differences in response timing between the groundwater level at most monitoring sites and streamflow. The mean CFC-based similarity based on the month-long groundwater levels and streamflow time series was not significantly correlated with any of the site characteristics, except the Euclidean distance to the outlet but the relationship was weak ($r_s = -0.40$, $p < 0.01$). The mean CFC-based similarity between each groundwater time series and the streamflow time series at the catchment outlet was significantly larger for sites with a TWI between 4 and 6 than for the other sites ($p = 0.002$). This difference was not significant for the sites with an upslope contributing area between 200 and 600 m^2, nor for the sites with a slope between 30 and 50% (Mann-Whitney $p = 0.054$ and 0.48, respectively), even though these are also topographic characteristics of midslope locations (see definition in section 2.3).

The standard deviation of the CFC-based similarity was about 4 times larger than for the DTW-based similarity (mean = 0.27, lower quartile = 0.26, median = 0.28, upper quartile = 0.30) and did not vary significantly

with upslope contributing area, slope, or TWI. The frequency distribution of the CFC-based similarity did not vary systematically with landscape position either: all sites had either a long tailed, positively or negatively skewed or a uniform distribution. These findings were similar when only considering the months with or without snow cover, the months of the growing, dormant, and spring seasons or the months of the individual years, separately. The mean CFC-based similarity, however, was different for the different seasons and was significantly higher for the months without snow cover than the months with snow cover ($p < 0.001$). The mean CFC-based similarity was also significantly different between the growing, dormant, and spring seasons (growing-dormant: $p < 0.01$, growing-spring: $p < 0.001$, dormant-spring: $p < 0.01$) and between the individual years, except for 2011 and 2012 ($p = 0.34$) and 2011 and 2014 ($p = 0.53$). The results for the median CFC-based similarity were similar to those of the mean CFC-based similarity.

3.2.3. Analysis of Variance

Analysis of variance (ANOVA) was performed to quantify the degree with which landscape position and spatial distance can explain the variability in the similarity between groundwater levels and streamflow. The joint effect of TWI (a measure of landscape position) and Euclidean distance to the catchment outlet (a measure of spatial distance) explained 63% ($p < 0.001$) of the spatial variability in the mean DTW-based similarity (i.e., the similarity of the groundwater dynamics of each monitoring site relative to the streamflow time series at the catchment outlet averaged for the 41 months). The partial effect of TWI in explaining the variance in mean DTW-based similarity was 55% ($p < 0.01$), while the Euclidean distance to the catchment outlet only explained 5% ($p < 0.05$) but was a significant factor. Using the distance to the nearest stream, instead of the Euclidean distance to the outlet in the ANOVA, led to similar results: (adjusted R^2 of the joint effect: 0.62 ($p < 0.001$), partial effect TWI: 53% ($p < 0.001$) and partial effect of distance to the nearest stream: 3% ($p = 0.03$)). Soil depth (adjusted R^2 of the partial effect: <1%, $p = 0.21$) and the forest percentage of the upslope contributing area (adjusted R^2 of the partial effect: <1%, $p = 0.95$) did not explain a significant portion of the variability in the mean DTW-based similarity when conditioned on TWI. The results were similar for the median DTW-based similarity.

The total explained variance in mean CFC-based similarity by TWI and Euclidean distance to the catchment outlet was only 11% ($p = 0.03$). The partial effect of the TWI in explaining the variance in mean CFC-based similarity was <1% and not significant ($p = 0.30$), while the partial effect of the Euclidean distance to the outlet was 12% and significant ($p < 0.01$). The distance to the nearest stream was not a significant explanatory variable of the variability in mean CFC-based similarity: (adjusted R^2 of the joint effect of TWI and distance to the nearest stream: −3% ($p = 0.74$), partial effect TWI: −1% ($p = 0.61$) and partial effect of distance to the nearest stream: −2% ($p = 0.64$). Negative explained variances mean that the explanatory variables explain less of the variation than random normally distributed variables would [*Legendre*, 2008]. Soil depth (adjusted R^2 of the partial effect: −2%, $p = 0.63$) and the forest percentage of the upslope contributing area (adjusted R^2 of the partial effect: −2%, $p = 0.57$) did not explain a significant portion of the variability in the mean CFC-based similarity when conditioned on TWI. Soil depth (adjusted R^2 of the partial effect: −2%, $p = 0.99$) and forest percentage of the upslope contributing area (adjusted R^2 of the partial effect: 2%, $p = 0.17$) were also not significant predictors when conditioned on the distance to the catchment outlet. Comparable results were obtained for the median CFC-based similarity.

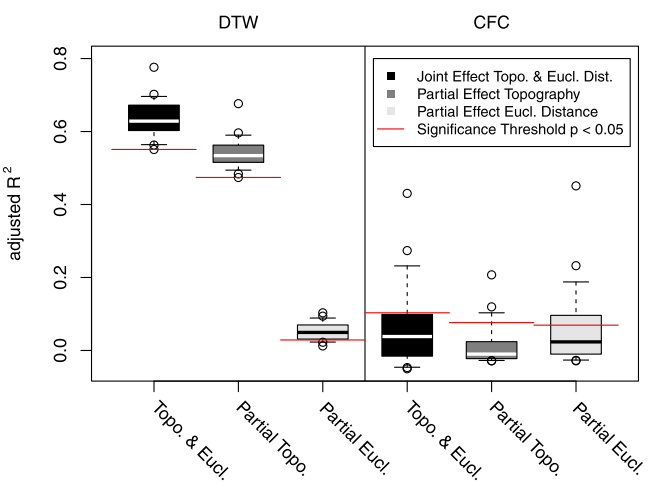

Figure 7. The explained variance of the DTW-based similarity (left) between the groundwater and streamflow time series for all 41 months is high for the joint effect of topography (Topographic Wetness Index) and Euclidean distance (black) and the partial effect of topography (dark gray) but small for the partial effect of Euclidean distance (light gray). The explained variance of the CFC-based similarity (right) is small for the joint and partial effect of topography and Euclidean distance. Red lines indicate a threshold above which adjusted R^2 values are considered significant.

In general, similar results were obtained for the ANOVA of the DTW- and CFC-based similarity when considering each of the 41 months individually (see Figure 7). The joint effect of TWI

and Euclidean distance to the catchment outlet on the percentage of explained variance in DTW-based similarity was high (lower quartile = 60%, median = 63%, upper quartile = 67%) and significant for all months, so was the partial effect of TWI (lower quartile = 52%, median = 53%, upper quartile = 56%). The partial effect of the Euclidean distance to the outlet on the explained variance in DTW-based similarity was much less (lower quartile = 3%, median = 5%, upper quartile = 7%) but significant for all months, except for July, August, and September 2011, May and August 2012, and April and May 2014. Results were similar when using the distance to the nearest stream, except that the partial effect of the distance to the nearest stream, in explaining the variability in DTW-based similarity was lower (lower quartile = 1%, median = 2%, upper quartile = 3%) and only significant for 4 months (2 months during the dormant season and 2 months during the growing season).

The joint effect of TWI and Euclidean distance to the outlet on the percentage of explained variance of CFC-based similarity for the individual months was low (lower quartile = −2%, median = 4%, upper quartile = 10%) and only significant for 9 out of the 41 months (Figure 7). The months for which the relation was significant occurred during all seasons (dormant: n = 4, spring: n = 4, growing: n = 1). The partial effect of the TWI on the percentage of explained variance of the CFC-based similarity was even less (lower quartile = −2%, median = −1%, upper quartile = 2%) and significant for only 5 out of 41 months (dormant: n = 2, spring: n = 3). The partial effect of Euclidean distance to the outlet on the fraction of explained variance in CFC-based similarity was slightly higher (lower quartile = −1%, median = 2%, upper quartile = 10%) and significant for 12 out of 41 months during all seasons (dormant: n = 4, spring: n = 4, growing: n = 4). The partial effect of the distance to the nearest stream in explaining the variability in CFC-based similarity was ≤0 (lower quartile = −2%, median = −1%, upper quartile = 0%) and not significant in any month.

In summary, the ANOVA results highlight the importance of topography in explaining the DTW-based similarity, while Euclidean distance to the outlet only explained a small fraction of the total variance in DTW-based similarity. The fraction of explained variance in CFC-based similarity by topography and Euclidean distance to the catchment outlet was much smaller and rarely significant. The distance to the nearest stream could only explain a small fraction of the variability in DTW-based similarity and was not significant for CFC-based similarity.

3.3. Similarity Between Groundwater Monitoring Sites

The interpolated mean DTW-based similarity between all pairs of monitoring sites was high for sites with similar topographic site characteristics and low for sites with contrasting topographic site characteristics. The interpolated mean DTW-based similarity was >0.8 when both groundwater monitoring sites had an upslope contributing area <300 m^2 or >700 m^2, a slope <30% or >40%, or a TWI <4 or >5 (see orange to red colors in Figure 8). Pairs of sites where one site has an upslope contributing area <300 m^2 and the other one >700 m^2, one site has a slope <30% and the other a slope >40% or one site has a TWI <4 and the other site a TWI >5 resulted in interpolated mean DTW-based similarity values <0.4 (see orange to yellow colors in Figure 8). The interpolated mean DTW-based similarity in groundwater dynamics between groundwater monitoring sites was not related to the distance to the nearest stream (see scatter of red, orange, and yellow colors in Figure 8d). There was also no clear relation between DTW-based similarity and the Euclidean distance between monitoring sites (see proportional circles in Figure 8). The results were generally similar when analyzing individual months or when using the interpolated median DTW-based

Table 2. Partial Mantel Test Statistics Examining the Partial, Linear Effect of the Interpolated Similarity in Site Characteristics (Upslope Contributing Area, Slope, and TWI) and the Interpolated Euclidean Distance Between Sites on the Interpolated Mean DTW-Based Similarity Between All Groundwater Monitoring Sites[a]

	Mean DTW		Mean CFC	
Predictor matrices | conditioned on	r_M	p	r_M	p
Upslope contributing area | Euclidean distance	0.04	0.17	0.47	<0.001
Euclidean distance | upslope contributing area	0.11	<0.001	0.11	0.03
Slope | Euclidean distance	0.51	<0.001	0.01	0.37
Euclidean distance | slope	0.11	<0.001	−0.16	0.99
Topographic Wetness Index | Euclidean distance	0.51	<0.001	0.25	<0.001
Euclidean distance | Topographic Wetness Index	0.02	0.29	0.03	0.26
Distance to the nearest stream | Euclidean distance	0.07	0.08	−0.16	0.98
Euclidean distance | distance to the nearest stream	−0.05	0.91	−0.19	0.99

[a] r_M: Mantel statistic based on Pearson's product-moment correlation. *p* values based on permutation test to quantify significance.

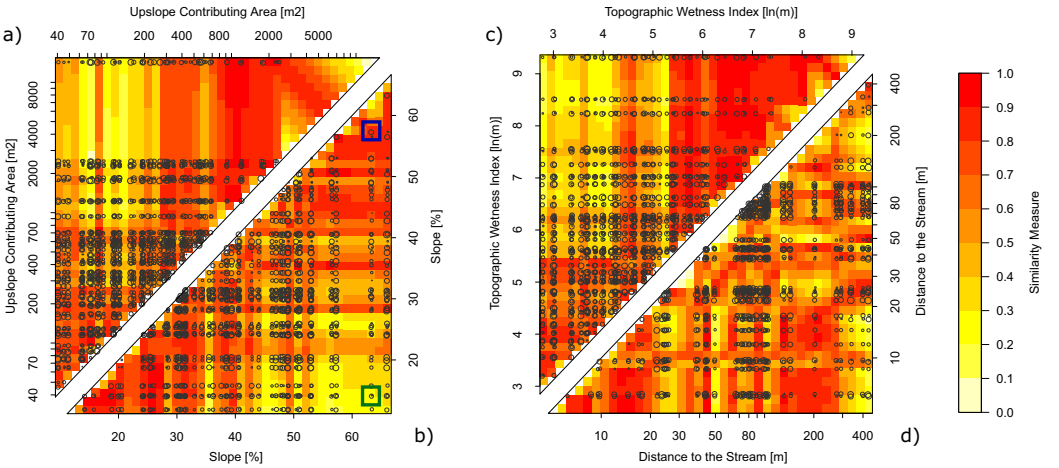

Figure 8. Interpolated mean DTW-based similarity among all groundwater monitoring sites show a systematic pattern (yellow to red colors) with upslope contributing area (upper left triangle), slope (lower left triangle), Topographic Wetness Index (upper right triangle) but not with distance to the nearest stream (lower right triangle) or the Euclidean distance between the groundwater wells (plotted as proportional circles). The groundwater similarity is color-coded from yellow (low) to red (high). For example, a site with a slope of 62% and a site with a slope of 58% had an interpolated DTW-based similarity of ~0.9 (see pixel marked in blue in Figure 8b). In contrast, a site with a slope of 62% and a site with a slope of 14% had a DTW-based similarity of ~0.2 (see pixel marked in green in Figure 8b).

similarity. Analyses of the interpolated mean or median CFC-based similarity did not show any systematic pattern and are therefore not shown here.

The comparison of groundwater similarity between the different groundwater monitoring sites using the Mantel statistics showed that the partial, linear effect of the interpolated similarity in most topographic indices (i.e., slope, TWI, and upslope contributing area) on the interpolated mean DTW-based and mean CFC-based similarity was higher than the partial, linear effect of the interpolated Euclidean distance between the monitoring sites (see Table 2). Soil depth (partial $r_M = -0.14$, $p = 0.99$) and the forest percentage of the upslope contributing area (partial $r_M = -0.02$, $p = 0.72$) were not significantly correlated with the interpolated mean DTW-based similarity. The same applied to the mean CFC-based groundwater similarity (soil depth partial $r_M = -0.15$, $p = 0.99$; forest percentage partial $r_M = 0.09$, $p = 0.05$). This is in agreement with the results of the analysis of the similarity between groundwater and streamflow. Similar results were obtained for the Mantel test statistics based on the interpolated median DTW-based similarity.

4. Discussion

4.1. Groundwater Similarity and Landscape Position

Our analyses showed that the spatial variability in distance-based groundwater similarity among the groundwater monitoring sites as well as between the groundwater monitoring sites and streamflow at the catchment outlet was strongly related to landscape position. For sites with a large upslope contributing area, high TWI and gentle slope (typically located at the footslopes) the groundwater dynamics were similar to streamflow (Figure 4a). In these locations, groundwater levels are typically shallow due to the lower gradient and large flux from upslope, so that only small amounts of rainfall are needed for the groundwater to respond. The effective porosity and saturated hydraulic conductivity in footslope locations can be lower than on the hillslopes due to deposition of finer soil material transported from mid and upslope locations [*Riecken and Poetsch*, 1960; *Rosenbloom et al*., 2001], which in general reduces drainage and sustains high initial water levels. In our catchment, we have no detailed data on soil texture to determine the effect of a change in texture on the groundwater dynamics. However, based on information on soil texture by *Schleppi et al*. [1998] and *Hagedorn et al*. [2000], the difference in texture of the two main gleysols in the catchment is small and therefore we assume that the influence of soil properties on groundwater dynamics is smaller than the effect of topography. The close proximity of most footslope sites to the stream and the similarity in their response dynamics can be interpreted as footslope sites contributing to streamflow during both baseflow and stormflow conditions.

In uphill sites with a small contributing area, low TWI, and steep slope, the groundwater dynamics differed from the streamflow dynamics (Figure 4a). The hydraulic gradient is typically high and soils are better drained, which leads to predominantly lower groundwater levels and higher storage capacities. During a rainfall event the available storage in the unsaturated zone first has to be satisfied before groundwater tables rise, which occurs therefore less frequent and is delayed relative to the streamflow response. This is reflected in the lower similarity between groundwater and streamflow and also suggests that steep uphill locations are most likely less frequently connected to the stream and if so, most likely contribute to streamflow on the falling limb of the hydrograph.

These differences in groundwater dynamics between footslope, midslope, and upslope locations are in agreement with previous studies in the same catchment [*Rinderer et al*., 2016] and hillslope studies at other sites [*Detty and McGuire*, 2010; *Penna et al*., 2015; *van Meerveld et al*., 2015; *Blumstock et al*., 2016] that showed a strong relation between the distance to the stream and the correlation between groundwater and streamflow response [*Seibert et al*., 2003; *Haught and van Meerveld*, 2011; *von Freyberg et al*., 2014]. However, in our study the relation between mean groundwater similarity relative to streamflow and the distances to the stream (either nearest stream or the outlet) was weaker than for TWI (and not significant for CFC based similarity for the distance to the nearest stream; Table 1). Most of the previous studies had their wells arranged on hillslopes adjacent to the stream and therefore the footslope sites automatically had the shortest distances to the stream and the uphill sites the longest distances to the steam. In our study, the monitoring sites were distributed across the entire catchment and therefore were less regularly aligned with respect to the distance to the nearest stream, which may cause the relation between groundwater similarity and landscape position or distance to the nearest stream to be less clear.

The high explained variability in distance-based groundwater similarity by topographic indices suggests that groundwater dynamics are strongly dependent on the setting in the landscape and cannot be studied independently from the upslope (contributing) and local (draining) conditions. This is also in agreement with studies that used distributed models to simulate streamflow and groundwater response of a catchment [*Ewen and Birkinshaw*, 2007; *Norbiato and Borga*, 2008; *Camporese et al*., 2014]. A challenge for all modeling and spatial data analysis studies is capturing the spatial heterogeneity of the input parameters and the spatial discretization of the model domain [*Paniconi and Putti*, 2015; *Rinderer and Seibert*, 2012]. This also applies to our analysis that originates from a 2 $\times$ 2 m LiDAR DEM but was deliberately coarsened to 6 $\times$ 6 m so that the slope better reflected the hydraulic gradient of the groundwater table and not the surface microtopography. The relations found in our study are expected to depend on the resolution of the DEM and we suggest choosing a spatial resolution that is appropriate for the characteristic length scale of groundwater (i.e., a few meters to tens of meters) [*Lyon et al*., 2006; *Bachmair et al*., 2012]. In our case the length scale of TWI was 21 m or ca. three pixels (semivariogram analysis performed as in *Western et al*. [1998]). This short length scale suggests that in a steep catchment with complex topography, distance-based interpolation methods will likely result in unrealistic spatial patterns of groundwater storage distribution when being applied beyond these distances, unless additional auxiliary variables are considered.

4.2. Is Landscape Position More Important Than Spatial Distance?

One key objective of this study was to investigate the relative strength of landscape position and spatial distance as predictors for similarity in shallow groundwater dynamics. ANOVA and partial Mantel tests showed that landscape position (represented by topographic indices) in general, explained more of the variability in distance-based similarity than either the Euclidean distance to the outlet (Figure 7) or the Euclidean distance between monitoring sites (Table 2 and Figure 8). When groundwater levels are predominantly close to the soil surface, slope is a proxy of the hydraulic gradient (assuming steady state flow conditions) and an indicator of local drainage, while the upslope contributing area is a proxy of the water inputs from upslope. From this it follows that TWI (defined as the ratio of upslope contributing area and slope) is a physically meaningful predictor of groundwater similarity that represents the ratio between water input and drainage at a point and therefore has successfully been used in conceptual modes to simulate catchment-scale patterns of groundwater dynamics.

Our study showed that neighboring sites, which were only a few meters to tens of meters apart from each other, could have very different groundwater dynamics (Figure 4a). The similarity in groundwater dynamics between groundwater monitoring sites was therefore more determined by similarity in site characteristics

than by the Euclidean distance between the monitoring sites (Figure 8). Despite differences in methodology, these results are in agreement with the similarity between wells and streamflow and the short characteristic length scales (in the order of 10–20 m) reported for groundwater variability in a hillslope study in the Catskill Mountains, New York State during the wet spring season when groundwater levels were high [*Lyon et al*., 2006]. It also agrees with findings from three hillslopes in Germany, where small-scale morphologic features influenced groundwater response variability [*Bachmair and Weiler*, 2012] and with measurements on the Panola hillslope near Atlanta (Georgia, USA) where wells only a few meters apart from each other could react very differently [*Tromp-van Meerveld and McDonnell*, 2006].

Soil depth was considered to be an additional important predictor variable for groundwater similarity in other studies [*Tromp-van Meerveld and McDonnell*, 2006; *Camporese et al*., 2014; *Penna et al*., 2015; *Gannon et al*., 2014] but was not statistically significant in explaining the variability in the DTW- and CFC-based groundwater similarity for this study catchment (Table 1, ANOVA and Mantel tests). This is most likely due to the high antecedent wetness conditions throughout the year and the low saturated hydraulic conductivity of the deeper soil layers that cause groundwater tables to perch at shallow soil depths, regardless of the actual depth of the soil. The forest percentage of the upslope contributing area was also not correlated with DTW- and CFC-based similarity but was correlated with topographic indices (Table 1). This suggests that forested areas are not found in the flat parts of the catchment because the groundwater level is persistently close to the soil surface, which limits the growth of deeper roots. While we think that vegetation can be an important control on groundwater and an indicator of groundwater similarity in other catchments with drier climatic conditions and better drained soils, our results suggest that in this catchment the spatial distribution of vegetation is not a dominant control on groundwater dynamics but rather a result of it [*Rinderer et al*., 2014].

Differences between the relative strength of the explanatory power of landscape position and spatial distance were smaller for the correlation-based similarity measure, which is expected to be sensitive to differences in groundwater response timing. The ANOVA results showed that the partial effect of topography and Euclidean distance to the catchment outlet on the explained variance in the correlation-based similarity was small (Figure 7). The correlation-based similarity was relatively uniform across the catchment, despite clear differences in site characteristics and landscape positions (Figure 4b). The predominantly wet antecedent conditions and the low drainable porosity in the study catchment could explain why groundwater at most monitoring sites and streamflow responded very frequently to rainfall events and showed only a relatively short delay [*Rinderer et al*., 2014, 2016]. The small spatial variability of CFC-based similarity for the monthlong time series is, however, contradictory to the results of *Rinderer et al*. [2016], who reported that event-based groundwater response timing was spatially variable and correlated with topographic indices. The median time to rise in their study was less than 35 min but the variability in median response times among sites was large (IQR: 5–105 min). A possible explanation for why CFC-based similarity did not appear to be very different for the different monitoring sites could be that these differences in timing during individual events were either too small to affect the similarity measure or were too variable and averaged out on the monthly and seasonal timescales considered in our study.

4.3. Does Groundwater Similarity Differ Between Seasons?

The CFC-based similarity measures captured seasonal differences in groundwater similarity that were not apparent from the DTW-based similarity. The CFC-based similarity values were higher during summer and lower during the winter, which suggests that groundwater and streamflow dynamics were more coupled during the summer than during the winter months. This seasonal variability in the coupling of groundwater and streamflow is partly in agreement with previous studies that reported the lowest correlations between groundwater levels and TWI during the dormant season [*Rinderer et al*., 2014]. This is when groundwater levels are lowest and most variable across the catchment, which probably results in a partial disconnection of the sites from their upslope contributing area and from the stream. Correlations between groundwater levels and TWI were higher during the spring and growing season when snowmelt or frequent rainstorms cause groundwater levels to be closer to the soil surface and upslope contributing areas are most likely better connected [*Rinderer et al*., 2014].

Other studies reported seasonal difference in the pattern of groundwater response in different landscape positions that were not identified in this study. For example, on three hillslopes in Germany groundwater

response was observed throughout the entire hillslope during the drier growing season but was limited to footslope locations during the winter [*Bachmair and Weiler*, 2012]. In the Hubbard Brook experimental forest, the median water levels in footslope and uphill locations were significantly different during the dry growing season but not during the wet dormant season [*Detty and McGuire*, 2010].

4.4. Highest Variability in Groundwater Similarity at Midslope Locations

Sites with topographic characteristics that are typical for midslope locations, such as a local slope between 30 and 50% (24 sites out of 51), an upslope contributing area between 200 and 600 m^2 (18 sites out of 51), or a TWI between 4 and 6 (27 sites out of 51) showed the largest variability in groundwater similarity relative to streamflow (Figures 1 and 5). The midslope locations with the range of TWI, slope, and upslope contributing area as stated above comprised 3.7 ha or 18% of the catchment area. This large variability in similarity suggests that the groundwater dynamics of midslope locations are most difficult to predict based on landscape characteristics, which agrees with results from other studies in mountainous catchments [*Camporese et al*., 2014; *Tetzlaff et al*., 2014]. The response behavior of these locations is most likely dominated by an interplay of factors comprising not only of static controls, such as topography (predominantly the flux of water from upslope as represented by the upslope accumulated area, and the drainage as represented by the local slope), effective porosity, and saturated hydraulic conductivity of the soil, but also dynamic controls, such as antecedent groundwater levels, rainfall characteristics, and hydrologic connectivity to upslope and downslope locations. This variability was also observed in other studies and highlights that midslope locations are most variable in terms of groundwater dynamics [*Rinderer et al*., 2014; *Tetzlaff et al*., 2014] and important in terms of catchment-scale hydrological connectivity [*Stieglitz et al*., 2003; *McNamara et al*., 2005; *Ocampo et al*., 2006; *van Meerveld et al*., 2015; *Jencso et al*., 2009]. The synchronicity in timing between the groundwater response at midslope locations with a TWI between 4 and 6 and the streamflow response (as highlighted by the significantly higher mean CFC-based similarity compared to other landscape positions) is a first (but not necessarily a causal) indicator of the importance of midslope locations as runoff source areas during events and catchment connectivity [*van Meerveld et al*., 2015; *McNamara et al*., 2005]. However, not every site, whose groundwater dynamic shows a high similarity with the streamflow time series at the catchment outlet, is necessarily also connected to the stream and contributes to streamflow [*Ambroise*, 2004; *Nippgen et al*., 2015].

5. Conclusions

This study investigated groundwater similarity based on month and season-long time series (rather than mean or median groundwater levels or event-based groundwater response time characteristics) across a small catchment with low-permeability soils to determine whether groundwater similarity is more related to landscape position or spatial distance. The study is to our knowledge the first to use groundwater and streamflow time series of a large number of monitoring sites and a long (41 month) observation period to quantify the similarity in groundwater dynamics across an entire catchment.

Our results showed that the distance-based similarity measure (calculated by the integral between two time series X(t) and Y(t) when $X(t) < Y(t)$ for all time steps) captured spatial differences in groundwater dynamics among different landscape position, such as footslope, midslope, and upslope locations. In contrast, the correlation-based similarity measures (calculated by the cross correlation between X(t) and Y(t) at lag = 0) were not related to landscape position but revealed seasonal differences in groundwater dynamics that were not apparent from the distance-based similarity measures.

Landscape position explained a larger portion of the variability in distance-based groundwater similarity across the catchment than spatial distance. This was particularly true for groundwater similarity relative to streamflow at the catchment outlet, but also for the similarity among groundwater monitoring sites.

Topographic indices, in particular TWI, were good predictors of distance-based groundwater similarity and can thus be used to upscale groundwater data from monitoring sites to obtain catchment-scale patterns of groundwater dynamics. However, the differences in the variability of groundwater similarity between landscape positions also suggest that upscaling is likely to be more uncertain for midslope locations than for footslopes or upslopes. In general, the use of topographic indices as auxiliary variables in interpolation

methods is expected to results in better interpolation of groundwater levels than solely distance-based interpolation methods.

The seasonal differences in correlation-based groundwater similarity suggests a stronger coupling and likely more widespread connectivity of the different parts of the catchment during the wet growing season than during the season with snow cover.

Our findings imply that measuring concepts need to consider the spatial organization of groundwater dynamics in a catchment in order to monitor the most representative sites. In catchments with steep terrain and shallow groundwater tables, a stratified sampling approach based on landscape position seems most suitable to capture catchment-scale groundwater storage variability.

Acknowledgments

Special thanks to the University of Zurich (Department of Geography, Hydrology & Climate) for funding the setup and maintenance of the hydrological monitoring network in the study site since 2010. Ellen Cerwinka, Jana Dusik, Benjamin Fischer, Peter Herrmann, Seraina Kauer, Nadja Lavanga, Claudia Müller, Stephan Müller, Stefan Plötner, Sandra Pool, Paribesh Pradhan, Sandra Schärer, Karl Steiner, Ivan Woodrich, and Mirjam Zehnder for field and lab assistance. We also thank the Swiss Federal Institute for Forest, Snow and Landscape Research WSL for meteorological data, as well as the OAK - Gemeinde Alpthal and the Canton of Schwyz - Amt für Natur, Jagd und Fischerei, for their cooperation. Groundwater and streamflow data are available from the authors upon request. Meteorological data can be requested from WSL. The authors gratefully acknowledge the financial support provided by the Swiss National Science Foundation (SNF) supporting the project: ICaRuS – Investigating Catchment Runoff Response by Assessing Spatial Patterns of Groundwater Dynamics.

References

Ali, G., C. Birkel, D. Tetzlaff, C. Soulsby, J. J. McDonnell, and P. Tarolli (2014), A comparison of wetness indices for the prediction of observed connected saturated areas under contrasting conditions, *Earth Surf. Processes Landforms*, *39*(3), 399–413.

Ali, G. A., C. L'Heureux, A. G. Roy, M.-C. Turmel and F. Courchesne (2011), Linking spatial patterns of perched groundwater storage and stormflow generation processes in a headwater forested catchment, *Hydrol. Processes*, *25*(25), 3843–3857.

Ambroise, B. (2004), Variable active versus contributing areas or periods: A necessary distinction, *Hydrol. Processes*, *18*(6), 1149–1155.

Anderson, M. G., and T. P. Burt (1978), The role of topography in controlling throughflow generation, *Earth Surf. Processes Landforms*, *3*, 331–334.

Asano, Y., T. Uchida, Y. Mimasu, and N. Ohte (2009), Spatial patterns of stream solute concentrations in a steep mountainous catchment with a homogeneous landscape, *Water Resour. Res.*, *45*, W10432, doi:10.1029/2008WR007466.

Bachmair, S., and M. Weiler (2012), Hillslope characteristics as controls of subsurface flow variability, *Hydrol. Earth Syst. Sci.*, *16*(10), 3699–3715.

Bachmair, S., M. Weiler, and P. A. Troch (2012), Intercomparing hillslope hydrological dynamics: Spatio-temporal variability and vegetation cover effects, *Water Resour. Res.*, *48*, W05537, doi:10.1029/2011WR011196.

Barling, R. D., W. Corporation, I. D. Moore, and B. Grayson (1994), A quasi dynamic wetness index for characterizing the spatial distribution of zones of surface saturation and soil water content, *Water Resour.*, *30*(4), 1029–1044.

Beven, K. J., and M. J. Kirkby (1979), A physically based, variable contributing area model of basin hydrology, *Hydrol. Sci. Bull.*, *24*(1), 43–69.

Blazkova, S., K. Beven, P. Tacheci, and A. Kulasova (2002), Testing the distributed water table predictions of TOPMODEL (allowing for uncertainty in model calibration): The death of TOPMODEL?, *Water Resour. Res.*, *38*(11), 1257, doi:10.1029/2001WR000912.

Bloemberg, T. G., J. Gerretzen, A. Lunshof, R. Wehrens, and L. M. C. Buydens (2013), Warping methods for spectroscopic and chromatographic signal alignment: A tutorial. *Anal. Chim. Acta*, *781*, 14–32.

Bloeschl, G., and R. Grayson (2000), Spatial observations and interpolation, in *Spatial Patterns in Catchment Hydrology: Observations and Modelling*, pp. 17–50, Cambridge University Press, Cambridge, U. K.

Blumstock, M., D. Tetzlaff, J. J. Dick, G. Nuetzmann, and C. Soulsby (2016), Spatial organisation of groundwater dynamics and streamflow response from different hydropedological units in a montane catchment, *Hydrol. Processes*, *30*, 3735–3753.

Burt, T. P., and D. P. Butcher (1985), Topographic controls of soil moisture distributions, *J. Soil Sci.*, *36*(1978), 469–486.

Buttle, J. M., P. W. Hazlett, C. D. Murray, I. F. Creed, D. S. Jeffries, and R. Semkin (2001), Prediction of groundwater characteristics in forested and harvested basins during spring snowmelt using a topographic index, *Hydrol. Processes*, *15*(18), 3389–3407.

Camporese, M., D. Penna, M. Borga, and C. Paniconi (2014), A field and modeling study of nonlinear storage-discharge dynamics for an Alpine headwater catchment, *Water Resour. Res.*, *50*, 806–822, doi:10.1002/2013WR013604.

Cleveland, W. S. (1979), Robust locally weighted regression and smoothing scatterplots, *J. Am. Stat. Assoc.*, *74*(368), 829–836.

Conrad, O. (2006), *Entwurf, Funktionsumfang, und Anwendung eines Systems für Automatisierte Geowissenschaftliche Analysen*, Univ. of Göttingen, Göttingen, Germany.

Detty, J. M., and K. J. McGuire (2010), Topographic controls on shallow groundwater dynamics: Implications of hydrologic connectivity between hillslopes and riparian zones in a till mantled catchment, *Hydrol. Processes*, *24*(16), 2222–2236.

Dhakal, A. S., and K. Sullivan (2014), Shallow groundwater response to rainfall on a forested headwater catchment in northern coastal California: Implications of topography, rainfall, and throughfall intensities on peak pressure head generation, *Hydrol. Processes*, *28*(3), 446–463.

Emanuel, R. E., A. G. Hazen, B. L. Mcglynn, and K. G. Jencso (2014), Vegetation and topographic influences on the connectivity of shallow groundwater between hillslopes and streams, *Ecohydrology*, *7*(2), 887–895.

Evans, S. (1980), An integrated system of terrain analysis and slope mapping, *Z. Geomorphol.*, *36*, supplement, 274–294.

Ewen, J., and S. J. Birkinshaw (2007), Lumped hysteretic model for subsurface stormflow developed using downward approach, *Hydrol. Processes*, *21*(11), 1496–1505.

Feyen, H., H. Wunderli, H. Wydler, and A. Papritz (1999), A tracer experiment to study flow paths of water in a forest soil, *J. Hydrol.*, *225*(3–4), 155–167.

Fischer, B. M. C., M. Rinderer, P. Schneider, T. Ewen, and J. Seibert (2015), Contributing sources to baseflow in pre-alpine headwaters using spatial snapshot sampling, *Hydrol. Processes*, *29*(26), 5321–5336.

Frisbee, M. D., C. J. Allan, M. J. Thomasson, and R. Mackereth (2007), Hillslope hydrology and wetland response of two small zero-order boreal catchments on the Precambrian Shield, *Hydrol. Processes*, *21*(22), 2979–2997.

Gannon, J., S. Baily, and K. J. McGuire (2014), Organizing groundwater regimes and response thresholds by soils: A framework for understanding runoff generation in a headwater catchment, *Water Resour. Res.*, *50*, 8403–8419, doi:10.1002/2014WR015498.

Giorgino, T. (2009), Computing and visualizing Dynamic Time Warping alignments in R: The dtw package, *J. Stat. Software*, *31*(7), 1–24.

Hagedorn, F., P. Schleppi, P. Waldner, and H. Flühler (2000), Export of dissolved organic carbon and nitrogen from Gleysol dominated catchments—The significance of water flow paths, *Biogeochemistry*, *50*, 137–161.

Haught, D. R. W., and H. J. van Meerveld (2011), Spatial variation in transient water table responses: Differences between an upper and lower hillslope zone, *Hydrol. Processes*, *25*(25), 3866–3877.

Inamdar, S. P., and M. J. Mitchell (2006), Hydrologic and topographic controls on storm-event exports of dissolved organic carbon (DOC) and nitrate across catchment scales, *Water Resour. Res.*, *42*, W03421, doi:10.1029/2005WR004212.
Jencso, K. G., and B. L. McGlynn (2011), Hierarchical controls on runoff generation: Topographically driven hydrologic connectivity, geology, and vegetation, *Water Resour. Res.*, *47*, W11527, doi:10.1029/2011WR010666.
Jencso, K. G., B. L. McGlynn, M. N. Gooseff, S. M. Wondzell, K. E. Bencala, and L. A. Marshall (2009), Hydrologic connectivity between landscapes and streams: Transferring reach-and plot-scale understanding to the catchment scale, *Water Resour. Res.*, *45*, W04428, doi:10.1029/2008WR007225.
Kosugi, K., S. Katsura, T. Mizuyama, S. Okunaka, and T. Mizutani (2008), Anomalous behavior of soil mantle groundwater demonstrates the major effects of bedrock groundwater on surface hydrological processes, *Water Resour. Res.*, *44*, W01407, doi:10.1029/2006WR005859.
Kosugi, K., M. Fujimoto, S. Katsura, H. Kato, Y. Sando, and T. Mizuyama (2011), Localized bedrock aquifer distribution explains discharge from a headwater catchment, *Water Resour. Res.*, *47*, W07530, doi:10.1029/2010WR009884.
Lana-Renault, N., D. Regüés, P. Serrano, and J. Latron (2014), Spatial and temporal variability of groundwater dynamics in a sub-Mediterranean mountain catchment, *Hydrol. Processes*, *28*(8), 3288–3299.
Legendre, P. (2008), Studying beta diversity: Ecological variation partitioning by multiple regression and canonical analysis, *J. Plant Ecol.*, *1*(1), 3–8.
Lyon, S. W., J. Seibert, A. J. Lembo, M. T. Walter, and T. S. Steenhuis (2006), Geostatistical investigation into the temporal evolution of spatial structure in a shallow water table, *Hydrol. Earth Syst. Sci.*, *10*, 113–125.
Mantel, N. (1967), The detection of disease clustering and a generalized regression approach, *Cancer Res.*, *27*(2), 209–220.
McDonnell, J. J. (1990), A rationale for old water discharge through macropores in a steep, humid catchment, *Water Resour. Res.*, *26*(11), 2821–2832.
McGlynn, B. L., and J. J. McDonnell (2003), Role of discrete landscape units in controlling catchment dissolved organic carbon dynamics, *Water Resour. Res.*, *39*(4), 1090, doi:10.1029/2002WR001525.
McGlynn, B. L., J. J. McDonnell, J. Seibert, and C. Kendall (2004), Scale effects on headwater catchment runoff timing, flow sources, and groundwater-streamflow relations, *Water Resour. Res.*, *40*, W07504, doi:10.1029/2003WR002494.
McMillan, H. K., and M. S. Srinivasan (2015), Characteristics and controls of variability in soil moisture and groundwater in a headwater catchment, *Hydrol. Earth Syst. Sci.*, *19*(4), 1767–1786.
McNamara, J. P., D. Chandler, M. Seyfried, and S. Achet (2005), Soil moisture states, lateral flow, and streamflow generation in a semi-arid, snowmelt-driven catchment, *Hydrol. Processes*, *19*(20), 4023–4038.
Metcalfe, R. A., and J. M. Buttle (2001), Soil partitioning and surface store controls on spring runoff from a boreal forest peatland basin in North-Central Manitoba, Canada, *Hydrol. Processes*, *15*(12), 2305–2324.
Mohn, J., Schürmann, A., and F. Hagedorn (2000), Increased rates of denitrification in nitrogen-treated forest soils, *For. Ecol. Manage.*, *137*, 113–119.
Moore, R. D., and J. C. Thompson (1996), Are water table variations in a shallow forest soil consistent with the TOPMODEL concept?, *Water Resour. Res.*, *32*(3), 663–669.
Mosley, M. P. (1982), Surface flow velocities through forest soils South Island, New Zealand, *J. Hydrol.*, *55*, 65–92.
Mosley, M. R. (1979), Streamflow generation in a forested watershed, New Zealand, *Water Resour. Res.*, *15*(4), 795–806.
Nielsen, N. P. V., J. M. Carstensen, and J. Smedsgaard (1998), Aligning of single and multiple wavelength chromatographic profiles for chemometric data analysis using correlation optimised warping, *J. Chromatogr. A*, *805*(1–2), 17–35.
Nippgen, F., B. L. McGlynn, and R. E. Emanuel (2015), The spatial and temporal evolution of contributing areas, *Water Resour. Res.*, *51*, 4550–4573, doi:10.1002/2014WR016719.
Norbiato, D., and M. Borga (2008), Analysis of hysteretic behaviour of a hillslope-storage kinematic wave model for subsurface flow, *Adv. Water Resour.*, *31*(1), 118–131.
Nychka, D., R. Furrer, J. Paige, and S. Sain (2016), *Fields-Package Reference Manual v8.3.6*, CRAN-Repository, Boulder, Colo., doi:10.5065/D6W957C.
O'Callaghan, J. F., and D. M. Mark (1984), The extraction of drainage networks from digital elevation data, *Comput. Vision Graphics Image Process.*, *28*(2), 323–344.
Ocampo, C. J., M. Sivapalan, and C. Oldham (2006), Hydrological connectivity of upland-riparian zones in agricultural catchments: Implications for runoff generation and nitrate transport, *J. Hydrol.*, *331*(3–4), 643–658.
Paniconi, C., and M. Putti (2015), Physically based modeling in catchment hydrology at 50: Survey and outlook, *Water Resour. Res.*, *51*, 7090–7129, doi:10.1002/2015WR017780.
Penna, D., N. Mantese, L. Hopp, M. Borga, and G. Dalla Fontana (2015), Spatio-temporal variability of piezometric response on two steep alpine hillslopes, *Hydrol. Processes*, *29*(2), 198–211.
Riecken, F., and E. Poetsch (1960), Genesis and classification considerations of some prairie-formed soil profiles from local alluvium in Adair County, Iowa, *Acad. Sci.*, *67*, 268–276.
Rinderer, M., and J. Seibert (2012), Soil information in hydrologic models: Hard data, soft data, and the dialog between experimentalists and modelers, in *Hydropedology— Synergetic Interaction of Soil Science and Hydrology*, edited by H. Lin, pp. 515–536, Elsevier B.V., Waltham, Mass.
Rinderer, M., I. van Meerveld, and J. Seibert (2014), Topographic controls on shallow groundwater levels in a steep, prealpine catchment: When are the TWI assumptions valid?, *Water Resour. Res.*, *50*, 6067–6080, doi:10.1002/2013WR015009.
Rinderer, M., I. van Meerveld, M. Stähli, and J. Seibert (2016), Is groundwater response timing in a pre-alpine catchment controlled more by topography or by rainfall?, *Hydrol. Processes*, *30*(7), 1036–1051.
Rodhe, A., and J. Seibert (2011), Groundwater dynamics in a till hillslope: Flow directions, gradients and delay, *Hydrol. Processes*, *25*, 1899–1909.
Rodhe, A., L. Nyberg, and K. Bishop (1996), Transit times for water in a small till catchment from a step shift in the oxygen 18 content of the water input, *Water Resour. Res.*, *32*(12), 3497–3511.
Rosenbloom, N. A., S. C. Doney, and D. S. Schimel (2001), Geomorphic evolution of soil texture and organic matter in eroding landscapes, *Global Biogeochem. Cycles*, *15*(2), 365–381.
Sakoe, H., and S. Chiba (1978), Dynamic programming algorithm optimization for spoken word recognition, *IEEE Trans. Acoustics Speech Signal Process.*, *26*(1), 43–49.
Schleppi, P., N. Muller, H. Feyen, A. Papritz, J. B. Bucher, and H. Flühler (1998), Nitrogen budgets of two small experimental forested catchments at Alptal, Switzerland, *For. Ecol. Manage.*, *101*, 177–185.

Seibert, J., and B. L. McGlynn (2007), A new triangular multiple flow direction algorithm for computing upslope areas from gridded digital elevation models, *Water Resour. Res.*, *43*, W04501, doi:10.1029/2006WR005128.
Seibert, J., K. Bishop, and L. Nyberg (1997), A test of TOPMODEL's ability to predict spatially distributed groundwater levels, *Hydrol. Processes*, *11*, 1131–1144.
Seibert, J., K. Bishop, A. Rodhe, and J. J. McDonnell (2003), Groundwater dynamics along a hillslope: A test of the steady state hypothesis, *Water Resour. Res.*, *39*(1), 1014, doi:10.1029/2002WR001404.
Sklash, M., M. Stewart, and A. Pearce (1986), Strom runoff generation in humid headwater catchments: 2. A case study of hillslope and low-order stream response, *Water Resour. Res.*, *22*, 1273–1282.
Skov, T., F. Van Den Berg, G. Tomasi, and R. Bro (2006), Automated alignment of chromatographic data, *J. Chemom.*, *20*(11–12), 484–497.
Smith, R. S., R. D. Moore, M. Weiler, and G. Jost (2014), Spatial controls on groundwater response dynamics in a snowmelt-dominated montane catchment, *Hydrol. Earth Syst. Sci.*, *18*(5), 1835–1856.
Smith, T., L. Marshall, and B. McGlynn (2014), Calibrating hydrologic models in flow-corrected time, *Water Resour. Res.*, *50*, 748–753, doi:10.1002/2013WR014635.
Stieglitz, M., J. Shaman, J. McNamara, V. Engel, J. Shanley, and G. W. Kling (2003), An approach to understanding hydrologic connectivity on the hillslope and the implications for nutrient transport, *Global Biogeochem. Cycles*, *17*(4), 1105, doi:10.1029/2003GB002041.
Tarboton, G. D. (1997), A new method for the determination of flow directions and upslope areas in grid digital elevation models, *Water Resour.*, *33*(2), 309–319.
Tetzlaff, D., C. Soulsby, S. Waldron, I. A. Malcolm, P. J. Bacon, S. M. Dunn, A. Lilly, and A. F. Youngson (2007), Conceptualization of runoff processes using a geographical information system and tracers in a nested mesoscale catchment, *Hydrol. Processes*, *1307*, 1289–1307.
Tetzlaff, D., C. Birkel, J. Dick, J. Geris, and C. Soulsby (2014), Storage dynamics in hydropedological units control hillslope connectivity, runoff generation, and the evolution of catchment transit time distributions, *Water Resour. Res.*, *50*, 969–985, doi:10.1002/2013WR014147.
Tiedeman, C. R., D. J. Goode, and P. A. Hsieh (1998), Characterizing a ground water basin in a new England mountain and valley terrain, *Ground Water*, *36*(4), 611–620.
Tobler, W. R. (1970), A computer movie simulation urban growth in detroit region, *Econ. Geogr.*, *46*(332), 234–240.
Tomasi, G., F. Van Den Berg, and C. Andersson (2004), Correlation optimized warping and Dynamic Time Warping as preprocessing methods for chromatographic data, *J. Chemom.*, *18*(5), 231–241.
Travis, M. R., W. D. Iverson, H. Gary, and C. G. Johnson (1975), VIEWIT: Computation of seen area, slope and aspect for land-use planning, *Tech. Rep. PSW 11*, USDA - For. Serv., Berkeley, Calif.
Troch, P. A., M. Mancini, C. Paniconi, and E. F. Wood (1993), Evaluation of a distributed catchment scale water balance model, *Water Resour.*, *29*(6), 1805–1817.
Tromp-van Meerveld, H. J., and J. J. McDonnell (2006), Threshold relations in subsurface stormflow: 2. The fill and spill hypothesis, *Water Resour. Res.*, *42*, W02411, doi:10.1029/2004WR003800.
van Meerveld, H. J., J. Seibert, and N. E. Peters (2015), Hillslope-riparian-stream connectivity and flow directions at the Panola Mountain Research Watershed, *Hydrol. Processes*, *29*(16), 3556–3574.
von Freyberg, J., D. Radny, H. E. Gall, and M. Schirmer (2014), Implications of hydrologic connectivity between hillslopes and riparian zones on streamflow composition, *J. Contam. Hydrol.*, *169*, 62–74.
Western, A. W., and R. B. Grayson (1998), The Tarrawarra data set: Soil moisture patterns, soil characteristics, and hydrological flux measurements, *Water Resour.*, *34*(10), 2765–2768.
Western, A. W., G. Bloeschl, and R. B. Grayson (1998), Geostatistical characterisation of soil moisture patterns in the Tarrawarra catchment, *J. Hydrol.*, *205*, 20–37.
Winter, T. C., D. C. Buso, P. C. Shattuck, P. T. Harte, D. A. Vroblesky, and D. J. Goode (2008), The effect of terrace geology on ground-water movement and on the interaction of ground water and surface water on a mountainside near Mirror Lake, New Hampshire, USA, *Hydrol. Processes*, *22*(1), 21–32.